RSC Advances

PAPER

View Article Online
View Journal | View Issue

Cite this: *RSC Adv.*, 2017, **7**, 53346

Investigating the tribological behavior of PEGylated MoS_2 nanocomposites as additives in polyalkylene glycol at elevated temperature

Zhuang Xu,[ab] Wenjing Lou,[a] Xinhu Wu,[ab] Xiaobo Wang *[a] and Junying Hao*[a]

Received 6th October 2017
Accepted 10th November 2017

DOI: 10.1039/c7ra10992j

rsc.li/rsc-advances

MoS_2–polydopamine–methoxypolyethyleneglycol amine (MoS_2–PDA–MGA) was synthesized through the combination of mussel-inspired chemistry and the Michael addition reaction. The modification of MoS_2 *via* PDA and MGA enhanced its dispersion stability in oil. The tribological properties of MoS_2–PDA–MGA for use as additives in polyalkylene glycol (PAG) base oil were investigated using an oscillating reciprocating tribometer at elevated temperatures. The results indicated that the addition of 0.7 wt% MoS_2–PDA–MGA in PAG resulted in excellent friction-reducing and anti-wear (AW) performances compared with PAG base oil. The tribological results of MoS_2–PDA–MGA and MoS_2 dispersed in PAG base oil after settling for 7 days indicate that MoS_2–PDA–MGA, with its good dispersion stability, has stable friction-reducing and AW properties. XPS analysis suggested that a protective boundary film formed on the wear surfaces during the friction and wearing process, which was believed to be responsible for the excellent tribological performance of MoS_2–PDA–MGA dispersed in PAG at elevated temperature.

1. Introduction

Almost all equipment requires the use of lubricating oil. Additives play a very important role in lubricating oils and are used to improve, modify or impart desired properties in base oils. However, the rapid development of industrial equipment requires lubricants to operate under severe conditions, such as high temperatures and high loads. In recent years, extensive research has been carried out on the application of nanomaterials as friction-reducing and AW additives.[1–5] Particularly, layered two-dimensional (2D) materials, such as molybdenum disulphide (MoS_2), tungsten disulphide (WS_2), hexagonal boron nitride (h-BN), and so on, have garnered tremendous attention in the lubrication field.[6–11] These materials, based on weak van der Waals forces, are capable of sliding between layers, and the formation of a tribo-film on the interface has been emphasized as the key mechanism for decreasing friction and wear. Due to the excellent tribological properties, MoS_2 and WS_2 have shown great potential for lubrication applications. For instance, Alazemi *et al.* investigated sub-micrometre-sized carbon spheres coated with a MoS_2 nanolayer (CS–MoS_2) as an additive in conventional oil lubricants (SAE 5W30) to improve the tribological properties.[12] Friction with 1 wt% CS–MoS_2 particle-containing oil was 15–35% lower compared to the base oil. Aldana *et al.* explored the mechanism of WS_2 nanoparticles with ZDDP additive in poly-alpha-olefin under the boundary lubrication regime. The results indicated that the AW performance of the ZDDP was enhanced when WS_2 nanoparticles were added to the system.[13]

Despite the excellent tribological properties of MoS_2/WS_2 nanomaterials, their development has been hindered by their poor dispersibility in lubricating oils. Fortunately, previous reports have shown that surface modification can improve the dispersion stability of nanomaterials in lubricating oil, and the modified nanomaterials exhibit significantly better friction-reducing and AW properties compared to the base oil.[14–19] Chen *et al.* synthesized oil-soluble ultrathin MoS_2 nanocomposites modified by oleylamine, and its addition could improve the load carrying property of liquid paraffin from less than 50 N to 2000 N at 120 °C.

Mussels display adhesive properties and have the ability to attach to almost all types of organic and inorganic surfaces, using dopamine (3,4-dihydroxy-phenylalanine) and other catechol compounds. Inspired by this property, dopamine undergoes oxidative self-polymerization under defined conditions, creating a polymerized layer on almost any type of material. Moreover, PDA film can act as a platform for easy and diverse secondary reactions to immobilize different functional groups.[20] Recently, surface modification of MoS_2-based materials by mussel-inspired dopamine chemistry and the Michael addition reaction has been studied.[21,22] Modified MoS_2 nanosheets consist of a core (MoS_2) and PEG chains densely tethered by a chemical bond on the MoS_2 surfaces. PEG contains polar groups and has good dispersibility in polar liquids, the special molecular structure allowed the modified MoS_2 to disperse well in polar liquids. However, the potential of PEGylated MoS_2 nanocomposites as additives for lubricating oils has never been demonstrated. Moreover, polyalkylene glycol (PAG) lubricants

[a]*State Key Laboratory of Solid Lubrication, Lanzhou Institute of Chemical Physics, Chinese Academy of Sciences, Lanzhou 730000, China. E-mail: wangxb@lzb.ac.cn*
[b]*University of Chinese Academy of Sciences, Beijing 100049, PR China*

are unique among synthetic lubricants due to their high oxygen content and inherent polarity. More advanced technologies will demand the application of PAG synthetic lubricants. Consequently, it is very important to study the tribological properties of nanomaterial additives in PAG.

To demonstrate this concept, we first synthesized PEGylated MoS_2 through a combination of mussel-inspired chemistry and the Michael addition reaction.[22] The resulting product (MoS_2–PDA–MGA) was characterized by various characterization techniques, and when dispersed in PAG, it demonstrated an excellent dispersion stability. Its tribological behaviors were studied by a ball-on-disk tribometer for steel/steel contact at elevated temperature. Furthermore, the lubrication mechanism of PAG lubricants with MoS_2–PDA–MGA was explored by X-ray photoelectron spectroscopy (XPS).

2. Experimental

2.1. Materials

MoS_2 was purchased from XFNANO Materials Tech Co., Ltd. (XF-184-1, Nanjing, China). Other feedstocks, including dopamine hydrochloride (DA, 98%), Tris-hydroxylmethylaminomethane (Tris, >99.9%), methoxypolyethylene glycol amine (MGA, MW: 2000 Da, 99.25%) were obtained from Aladdin (Shanghai, China). Polyalkylene glycol (PAG) was obtained from Weier Chemical Corporation (Nanjing, China), and its typical properties are presented in Table 1. Deionized (DI) water was used in the whole experiment process. All chemical reagents were used without any further purification.

2.2. Synthesis of MoS_2–PDA–MGA

MoS_2–PDA–MGA was synthesized according to the procedures described by Zeng *et al.*,[22] with some modifications.

First, 300 mg MoS_2 was dispersed in 100 ml of a 5 g l^{-1} dopamine solution. Then, 1 ml of 1 M Tris buffer solution was added and stirred for 6 h at room temperature. After that, the product was separated by centrifuging at 6000 rpm for 10 min. It was then washed with water and ethanol several times and dried under vacuum at 60 °C to obtain the MoS_2–PDA (MoS_2 coated with polydopamine (PDA) thin films).

Second, 200 mg of MoS_2–PDA was first dispersed in 100 ml of Tris buffer solution (10 mM, pH = 8.5), 300 mg of MGA was added into the reaction system, and this reaction was carried out at room temperature (25 °C) for 12 h. The final product was separated by centrifuging at 6000 rpm for 10 min, washed with water and ethanol several times to remove the unreacted polymers and dried at 50 °C for 12 h. MoS_2–PDA–MGA was obtained.

Table 1 Physicochemical properties of PAG base oil

Item	Value
Kinematic viscosity at 40 °C ($mm^2\ s^{-1}$)	98.64
Kinematic viscosity at 100 °C ($mm^2\ s^{-1}$)	18.48
Viscosity index (VI)	209
Pour point (°C)	−40
Flash point (°C)	220
Acid value (mg KOH g^{-1})	0.05

2.3. Characterizations and measurements

X-ray diffraction (XRD) patterns were collected by a Bruker AXS D8-ADVANCE diffractometer. The morphology of MoS_2–PDA–MGA was obtained by a JEOL TEM-2100 Plus high-resolution transmission electron microscope (HRTEM) and a scanning electron microscope (SEM, HITACHI S-4800) equipped with an energy dispersive X-ray (EDX) detector. The Fourier transform infrared (FT-IR) spectra were collected on a Bruker Tensor 27 FT-IR spectrometer using the KBr disk method. The thermogravimetric analysis (TGA) was carried out on a TGA Netzsch STA 449 F5 instrument from ambient temperatures to approximately 650 °C with a heating rate of 10 °C min^{-1} in N_2 flow. The dispersion stability of MoS_2–PDA–MGA in PAG base oil was investigated using an ultraviolet-visible light (UV-vis) spectrophotometer (PERSEE, TU-1810) at different time intervals.

The tribological properties of MoS_2–PDA–MGA as an additive were evaluated by an Optimal SRV-IV oscillating reciprocating. The upper ball (ø 10 mm, AISI 52100 bearing steel, hardness 700 HV, surface roughness R_a = 25 nm) slides reciprocally against the stationary lower steel discs (AISI 52100 bearing steel, ø 24.00 × 7.88 mm, hardness of approximately 625 HV, surface roughness R_a = 41 nm). The wear volumes of the lower discs were measured using a MicroXAM-3D non-contact surface mapping profilometer. The morphology state and chemical composition of the wear scar surfaces were analysed by scanning electron microscopy (SEM, JSM-5600LV) and X-ray photoelectron spectroscopy (XPS, Thermos scientific, ESCALAB 250Xi).

3. Results and discussion

3.1. XRD, HR-TEM and EDS analysis of MoS_2–PDA–MGA

The XRD patterns of MoS_2–PDA–MGA and MoS_2 are shown in Fig. 1(a), and the characteristic peaks located at 14.25, 32.7, 35.95, 39.5, 49.8, 58.35, 60.36 and 72.8 are attributed to the (002), (100), (102), (103), (105), (110), (008) and (203) planes of MoS_2, respectively (PDF37-1492). The peak of MoS_2–PDA–MGA is consistent with MoS_2. The size distribution of MoS_2–PDA–MGA is shown in Fig. 1(b). The data were obtained by sampling a relevant number of particles and measuring the dimensions by FE-SEM. Their mean diameter is approximately 900 nm.

The morphologies of MoS_2 and MoS_2–PDA–MGA were characterized by HRTEM, as shown in Fig. 2. Fig. 2(a) and (b) show the low-magnification TEM images, and Fig. 2(c) is the magnified TEM images from Fig. 2(b). Compared with the morphology of the MoS_2, a thick organic film could be obviously observed in MoS_2–PDA–MGA. Fig. 2(d) shows the HRTEM image of the latter, and it is clear that there are three regions with different lattice fringes: MoS_2 (e2), organic layer (e1), and amorphous carbon film (e0). In addition, HRTEM displays the hexagonal lattice structure of the MoS_2, giving a lattice spacing of 0.27 nm (inset in Fig. 2(d), the areas were marked by black box in Fig. 2(d)). Therefore, the results clearly show that the MoS_2 have been successfully modified with PDA and MGA.

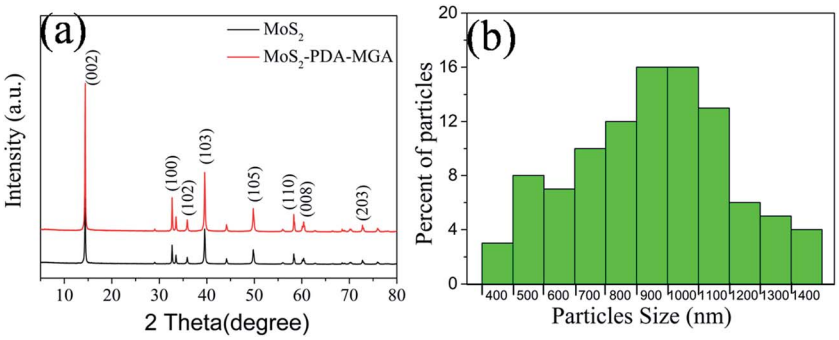

Fig. 1 XRD patterns and size distribution of MoS_2–PDA–MGA.

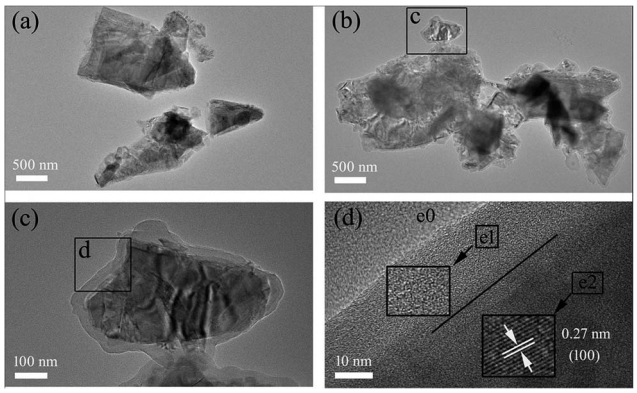

Fig. 2 TEM images of MoS_2 and MoS_2–PDA–MGA: (a) MoS_2, (b–d) MoS_2–PDA–MGA.

Furthermore, the EDS element mapping (Fig. 3) analysis of MoS_2–PDA–MGA displayed a homogeneous distribution of elemental C, O, N, Mo and S. It is clear that C, O and N appeared on the MoS_2–PDA–MGA. Thus, MoS_2–PDA–MGA was successfully synthesized.

3.2. FT-IR spectra and thermal properties of MoS_2–PDA–MGA

To further confirm structure and surface state of MoS_2–PDA–MGA, it was characterized by FT-IR and TGA. The FT-IR spectra of MoS_2 and MoS_2–PDA–MGA are shown in Fig. 3 and the main absorption peaks of MoS_2–PDA–MGA are all present in the IR spectra. Compared with the spectrum of the MoS_2, the new absorption peak at approximately 3450 cm^{-1} corresponds to the –OH and N–H stretching vibration. The absorption bands located at 1500 cm^{-1} and 1600 cm^{-1} are attributed to the aromatic rings and –C=C–, suggesting that PDA has been grafted on the MoS_2 surface. Moreover, the obvious peak at 1080 cm^{-1} assigned to the stretching vibration of C–O demonstrates that the polymer (MGA) is present on the surface of MoS_2. Consequently, these results indicate that MoS_2 was successfully modified with PDA and MGA.

Fig. 4 shows their TGA curves. Moreover, the weight percentage of polymer on the surface of MoS_2 was calculated. It

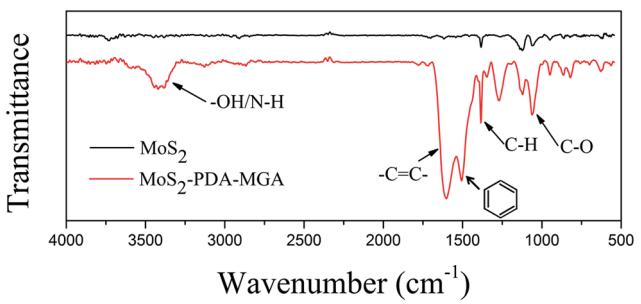

Fig. 4 The FTIR spectra of MoS_2 and MoS_2–PDA–MGA.

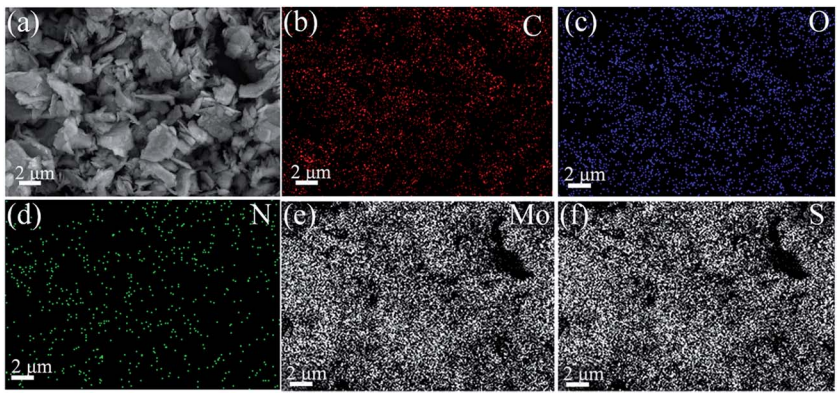

Fig. 3 FE-SEM image (a) of MoS_2–PDA–MGA and the corresponding element mapping for (b) C, (c) O, (d) N, (e) Mo and (f) S.

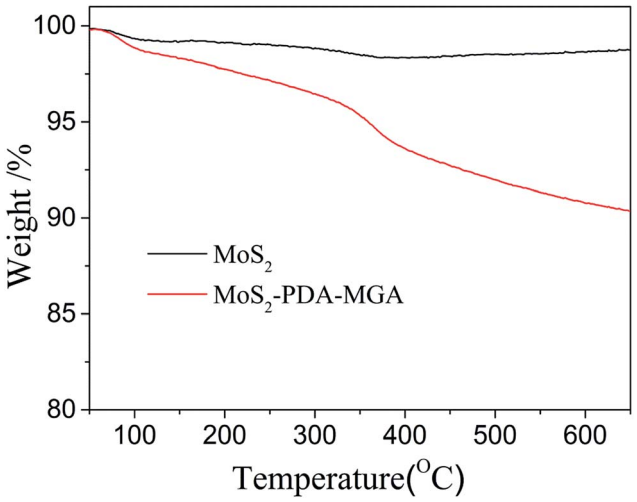

Fig. 5 Thermogravimetric curves of MoS_2 and MoS_2–PDA–MGA.

could be found that the weight loss of MoS_2 and MoS_2–PDA–MGA is 0.9% and 10.1%, respectively. The figures show that the weight percentage of polymer is approximately 9.2%. It is obvious that MoS_2 was modified with PDA and MGA (Fig. 5).

The dispersion stability of MoS_2 and MoS_2–PDA–MGA in PAG base oil has been estimated using pictures and UV-vis spectrophotometer. For comparison, a hybrid lubricant with 0.7 wt% MoS_2 was prepared as well. As shown in Fig. 6(a3), MoS_2–PDA–MGA retained good stability in PAG oils for two weeks after preparation. In contrast, the MoS_2 dispersion had the apparent precipitation after settling for 7 days (Fig. 6(b2)). Moreover, a large amount of MoS_2 precipitate was observed after settling for 15 days (Fig. 6(b3)). The variation of the relative concentration of the sample with time also demonstrates the excellent stability of MoS_2–PDA–MGA in the base oil (Fig. 6(d)). After 15 days, the relative concentration of MoS_2–PDA–MGA remained at 86.6%. However, the relative concentration of the MoS_2 suspensions in the oil significantly decreased with increasing settling time and was only at 8.9% after 15 days. The results indicate that MoS_2–PDA–MGA has better dispersion stability than MoS_2.

3.3. Tribological properties of MoS_2–PDA–MGA

The friction-reducing and AW performances of MoS_2–PDA–MGA as an additive in PAG were investigated for steel/steel contact under different loads at 150 °C. The duration for each test was 30 min, as shown in Fig. 7(a) and (b). The average friction coefficients decreased continuously with increasing MoS_2–PDA–MGA content. When the content of MoS_2–PDA–MGA reached to 0.7 wt%, the lubricant had the lowest average friction coefficient (Fig. 7(a)). However, further increasing the content above 0.7 wt% demonstrated that the friction coefficient could not be further improved. It can be concluded that, at a low concentration of MoS_2–PDA–MGA, the lubricant cannot sufficiently form an adequate tribo-film to prevent direct contact of the friction pairs, thereby leading to a relatively high friction coefficient and high wear. When the additive concentration was 0.7 wt%, MoS_2–PDA–MGA could form a sufficient tribo-film to provide optimum friction-reducing and AW properties. After the contact area becomes saturated with the tribo-film, further tribo-film formation would not be effective.[23] The addition of 0.7 wt% MoS_2–PDA–MGA could reduce the average friction coefficients to approximately 3.16%, 12.5% and 12.2%

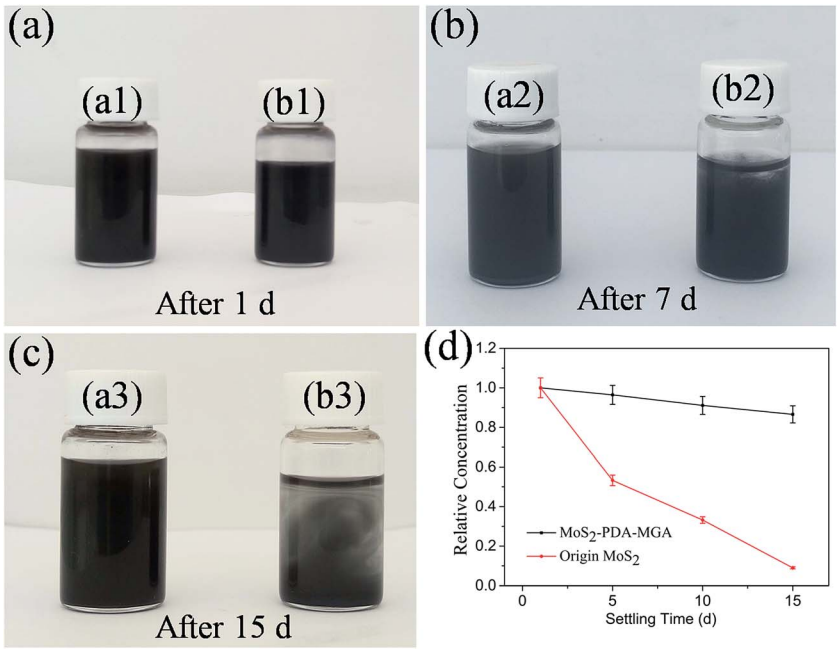

Fig. 6 Dispersion stabilities of MoS_2–PDA–MGA in the base oil. Camera pictures of MoS_2–PDA–MGA ((a1–a3)) and MoS_2 ((b1–b3)) dispersed in PAG base oil at different settling times; (d) dispersion stabilities of MoS_2–PDA–MGA in PAG oil determined by UV-vis spectrophotometer.

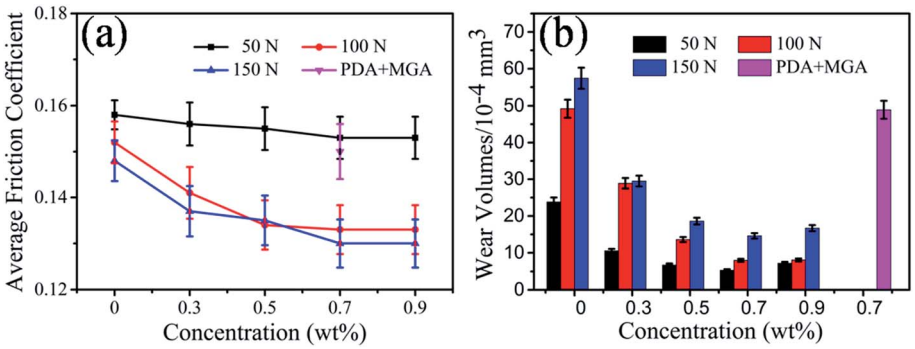

Fig. 7 Average friction coefficient and wear volumes of the discs lubricated by PAG and PAG containing MoS_2–PDA–MGA with different concentrations under various loads (temperature, 150 °C; stroke, 1 mm; frequency, 25 Hz).

compared with the base oil under loads of 50 N, 100 N and 150 N, respectively. In addition, PAG containing 0.7 wt% MoS_2–PDA–MGA also exhibits the lowest wear loss during the sliding process (Fig. 7(b)). In fact, the AW properties of the PAG base oil were improved by approximately 77.6%, 83.7% and 70.9% under loads of 50 N, 100 N and 150 N, respectively. Based on these values, it can be concluded that the addition of 0.7 wt% MoS_2–PDA–MGA in PAG is the optimum amount to provide significant friction reduction and AW properties for steel/steel contacts under a load of 100 N at 150 °C. Moreover, the effects of PDA and MGA on the tribological properties of PAG were also investigated, the results indicate that the tribological properties of PAG containing 0.7 wt% organics (0.35 wt% PDA and 0.35 wt% MGA) are similar to those of the PAG base oil under a load of 100 N at 150 °C, with no obvious improvement (Fig. 7(a) and (b)).

To investigate the effect of dispersion stability of nano-additives on the tribological properties, the tribological performance of MoS_2–PDA–MGA and MoS_2 dispersed in PAG base oil after settling over different time intervals were evaluated under a load of 100 N at 150 °C. All tests were carried out at an optimized concentration (0.7 wt%). As shown in (Fig. 8(a) and (b)), after settling 1 day, the friction coefficient and wear volumes of the MoS_2–PDA–MGA and MoS_2 dispersed in PAG base oil were similar. However, after settling for 7 days, the friction coefficient and wear volumes of MoS_2 dispersed in PAG base oil increased significantly. In contrast, the friction coefficient and wear volumes of MoS_2–PDA–MGA dispersed in PAG base oil were almost unchanged compared to the sample left to settle for 1 day. These results indicate that MoS_2–PDA–MGA, with its good dispersion stability, has stable friction-reducing and AW properties after settling for 7 days. The excellent tribological performances of MoS_2–PDA–MGA can be explained by the fact that MoS_2–PDA–MGA, with its good dispersion stability in PAG base oil, is able to easily access the contact interface and form an effective film that leads to a low friction coefficient and low wear volumes.

Then, the friction-reducing and AW properties of PAG containing MoS_2–PDA–MGA with optimized concentration (0.7 wt%) were further studied at various temperatures under a constant load of 100 N. As shown in Fig. 9(a), the average friction coefficient of 0.7 wt% MoS_2–PDA–MGA added in PAG demonstrated almost no change compared to the base oil at 50 °C. However, 0.7 wt% MoS_2–PDA–MGA in PAG dramatically improved the friction-reducing properties of the system as the temperature increased from 90 °C to 170 °C. For example, 0.7 wt% MoS_2–PDA–MGA reduced the friction coefficient by approximately 6.52% at 90 °C, 10.73% at 130 °C, 12.5% at 150 °C, and 12.0% at 170 °C. Furthermore, increasing the temperature may play an active role in improving the friction-

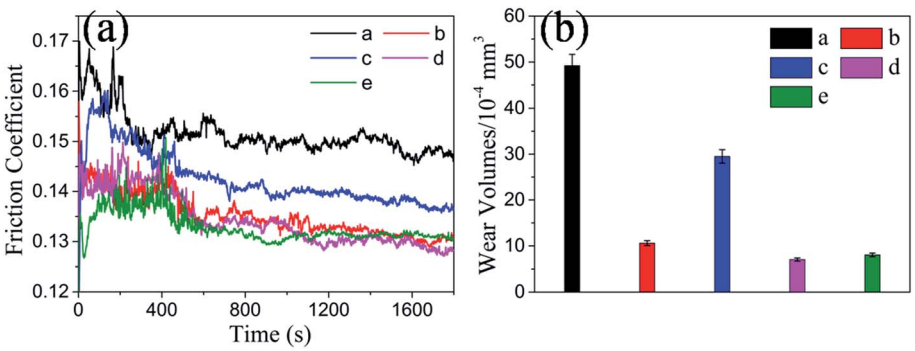

Fig. 8 Friction coefficient and wear volumes of the discs lubricated by PAG and PAG containing different additives (SRV load, 100 N; temperature, 150 °C; stroke, 1 mm; frequency, 25 Hz). (a) PAG; (b, c) 0.7 wt% MoS_2 dispersed in PAG base oil after settling 1 and 7 days; (d, e) 0.7 wt% MoS_2–PDA–MGA dispersed in PAG base oil after settling 1 and 7 days.

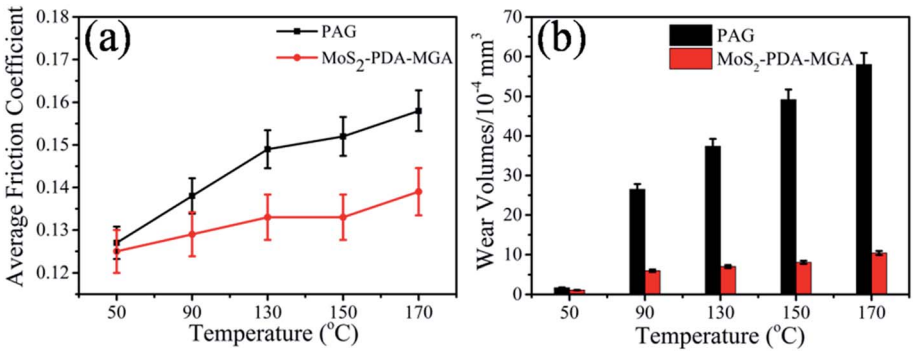

Fig. 9 Average friction coefficient and wear volumes of the discs lubricated by PAG and PAG containing 0.7 wt% MoS_2–PDA–MGA at various temperatures (SRV load, 100 N; stroke, 1 mm; frequency, 25 Hz).

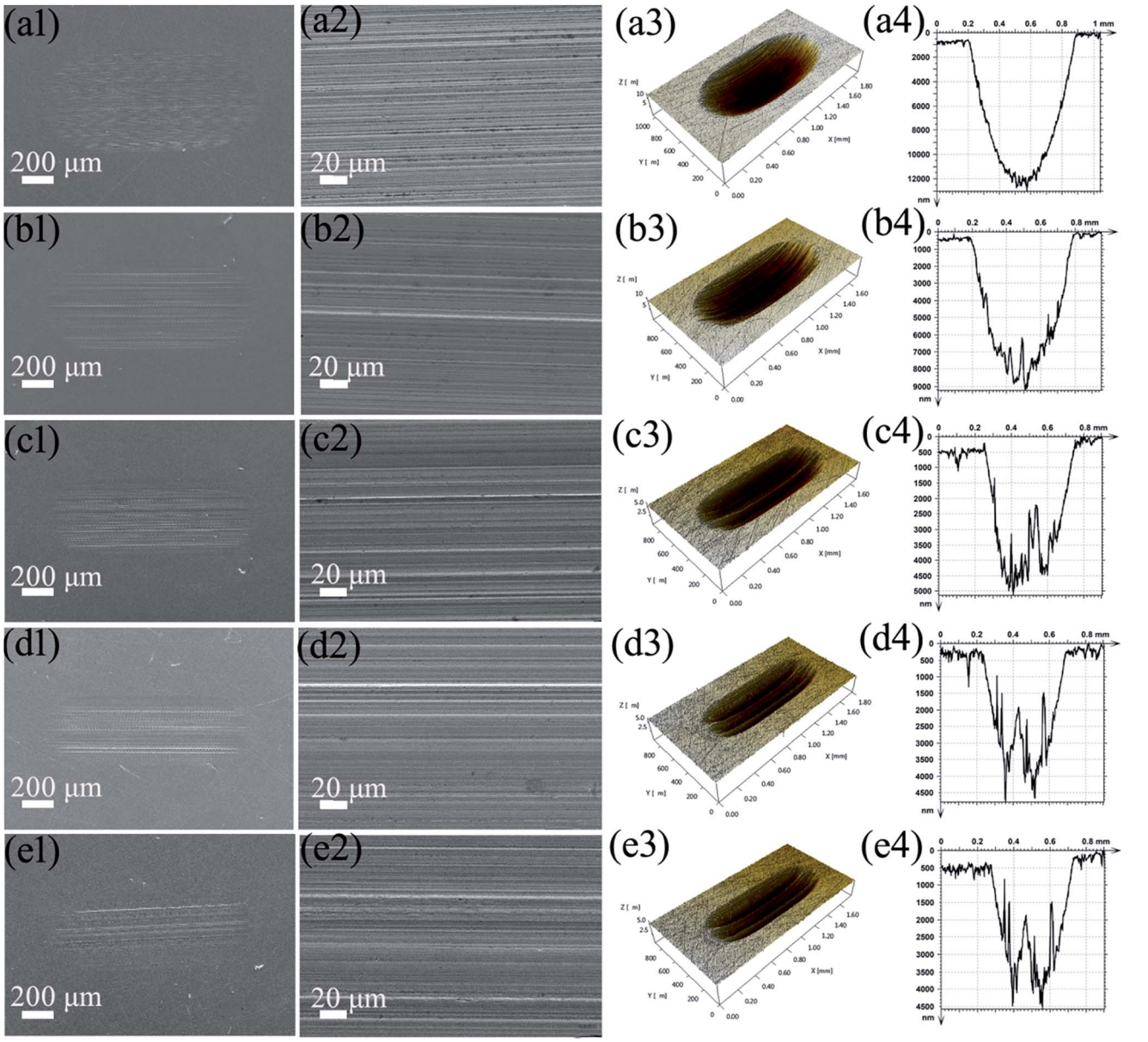

Fig. 10 SEM images and 3D optical microscopic images of the worn scar surfaces lubricated by PAG oil ((a1–a4)) and with different concentrations (0.3 wt% (b1–b4), 0.5 wt% (c1–c4), 0.7 wt% (d1–d4), 0.9 wt% (e1–e4)) of MoS_2–PDA–MGA under a load of 100 N (temperature, 150 °C; stroke, 1 mm; frequency, 25 Hz).

reducing of PAG with the additives.[24] The addition of MoS_2–PDA–MGA in PAG may form a lubrication film that maintains lower friction when the temperature is increased. Moreover, as shown in Fig. 9(b), compared with the base oil, the addition of 0.7 wt% MoS_2–PDA–MGA could reduce the wear volume by approximately 35.3%, 77.4%, 81.3%, 82.1%, and 83.7% at 50 °C, 90 °C, 130 °C, 150 °C, and 170 °C, respectively. This result indicates that the percentage of wear volume reduction increased when the temperature increased from 50 °C to 170 °C. Considering the results mentioned above, MoS_2–PDA–MGA added in PAG exhibits excellent friction-reducing and AW properties at elevated temperature, which might be due to the fact that raising the temperature played an active role in improving the tribological behavior of the base oil in the

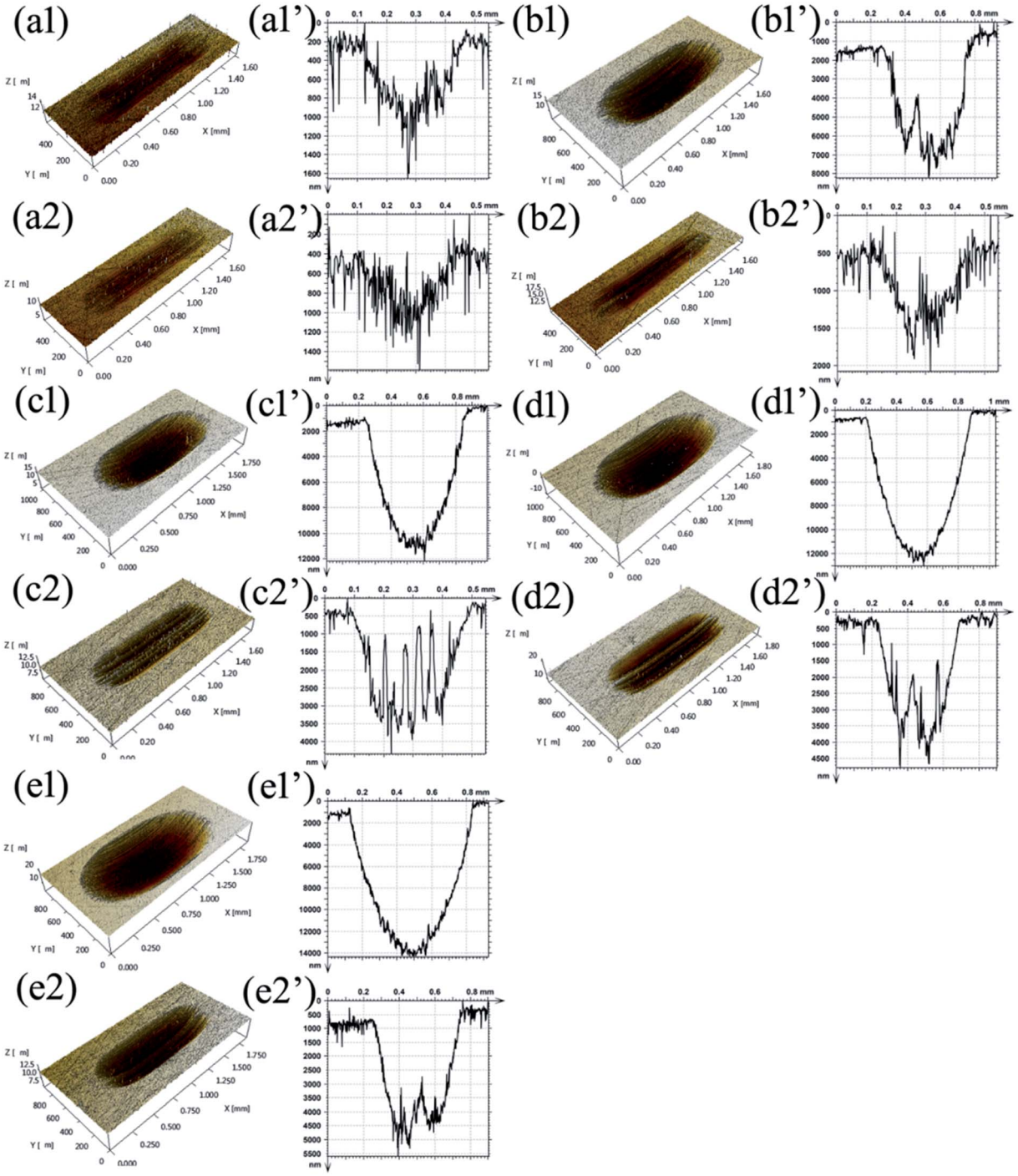

Fig. 11 3D optical microscopic images of wear scars lubricated by PAG ((a1), (a1′), (b1), (b1′), (c1), (c1′), (d1), (d1′), (e1), (e1′)) and PAG containing 0.7 wt% MoS_2–PDA–MGA ((a2), (a2′), (b2), (b2′), (c2), (c2′), (d2), (d2′), (e2), (e2′)) under 100 N at various temperatures: (a1), (a1′), (a2), (a2′) at 50 °C; (b1), (b1′), (b2), (b2′) at 90 °C; (c1), (c1′), (c2), (c2′) at 130 °C; (d1), (d1′), (d2), (d2′) at 150 °C; (e1), (e1′), (e2), (e2′) at 170 °C.

presence of nanoparticle additives.[24] Under higher temperature, thermal activation may promote the chemical reaction between MoS_2–PDA–MGA and the interfaces, which is more conducive to the formation of lubricating film.[25]

Fig. 10 shows SEM images and a 3D profile curve of the wear surfaces lubricated by PAG and PAG with different concentrations of MoS_2–PDA–MGA under loads of 100 N at 150 °C. It could be seen that the wear scar is wide and deep when the wear surfaces were lubricated by only PAG base oil, which indicates that severe wear has occurred. The surface of the friction pair lubricated by the PAG lubricants containing MoS_2–PDA–MGA was much narrower and much shallower than that lubricated with PAG base oil, especially when the percentage of MoS_2–PDA–MGA is 0.7 wt%, the lowest wear is obtained. Those results are consistent with the results in Fig. 7(b). The results indicate that MoS_2–PDA–MGA obviously enhanced the AW performance of PAG base oil, which is consistent with the wear volume results in Fig. 7(b). However, there were a few parallel grooves on the worn surfaces lubricated by PAG lubricants containing MoS_2–PDA–MGA, which might be due to the presence of a few nanocomposite aggregates. When the MoS_2–PDA–MGA were added into the PAG base oil, the additives tended to form a few aggregates and did not properly fill the furrows between the contact surfaces, and so, the parallel grooves increased in depth.[25,26]

Fig. 11 also shows the 3D morphologies and 3D profile curves of wear scars lubricated by PAG and PAG containing 0.7 wt% MoS_2–PDA–MGA at various temperatures under a load of 100 N. It is clear that the PAG lubricants containing MoS_2–PDA–MGA displayed smaller and shallower wear scars than the PAG base oil at elevated temperature. This result further confirms that the addition of MoS_2–PDA–MGA significantly enhanced the AW property of PAG base oil.

The worn surface of the discs lubricated by PAG containing 0.7 wt% MoS_2–PDA–MGA or MoS_2 (0.7 wt%) after different settling time intervals were characterized by XPS to explore the friction-reducing and AW mechanism. The chemical composition of the wear scar is shown in Fig. 12. After settling for 1 day, compared with the worn surface lubricated by MoS_2–PDA–MGA, the XPS spectra of the worn surfaces lubricated by MoS_2 showed no significant difference. However, after settling for 7 days, the peaks of Mo 3d and S 2p of the worn surfaces lubricated by MoS_2 were significantly reduced. This result corresponds to the results that show the significant increase in the friction coefficient and wear volumes of MoS_2 dispersed in PAG base oil after settling 7 days (Fig. 8). The XPS peaks of O 1s were located at approximately 529.5 eV and 532.4 eV (Fig. 12(a)), corresponding to FeO or Fe_2O_3, FeOOH, $FeSO_4$ or $Fe_2(SO_4)_3$, and C–O bonding.[27] The Fe 2p peaks appeared at binding energies of 710.3 eV and 724.4 eV (Fig. 12(b)), demonstrating that Fe_2O_3 and $Fe_2(SO_4)_3$ formed during the tribo-chemical reactions. The peaks at 233.3 eV and 232.3 eV of the friction surface are attributed to Mo 3d of MoS_2 and MoO_3 (Fig. 12(c)), indicating that MoS_2–PDA–MGA was absorbed on the friction pair surfaces and were partially oxidized during the sliding process to form MoO_3. The peaks of S 2p emerged at the binding energy of 168.6 eV (Fig. 12(d)),[28] which proves that $FeSO_4$ or $Fe_2(SO_4)_3$ was formed at the friction surface. These results confirmed that MoS_2–PDA–MGA, with its good dispersion stability, has stable friction-reducing and AW properties. XPS results suggest the deposition of MoS_2–PDA–MGA lamellae. Deposited MoS_2–PDA–MGA is speared on the contact interfaces and the weak van der Waals interaction between atomic lamellae of MoS_2–PDA–MGA facilitates their sliding on the friction interfaces. Therefore, MoS_2–PDA–MGA plays an important role in friction-reducing

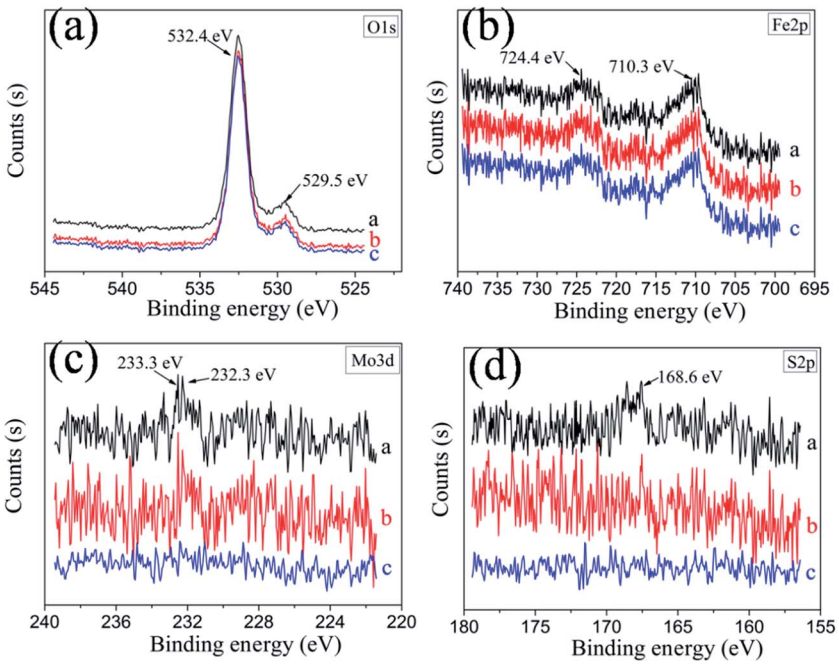

Fig. 12 XPS spectra of wear surfaces on the discs lubricated by PAG containing different additives under a load of 100 N at 150 °C. (a) 0.7 wt% MoS_2–PDA–MGA dispersed in PAG base oil after settling 1 day; (b, c) 0.7 wt% MoS_2 dispersed in PAG base oil after settling 1 and 7 days.

and AW properties.[11] On the other hand, MoS_2–PDA–MGA participated in a tribo-chemical reaction during the sliding process, and the boundary adsorption film and tribo-chemical reaction film were formed on the worn surfaces of the discs. The lubrication film can improve the friction-reducing and AW properties of PAG base oil.

4. Conclusions

MoS_2–PDA–MGA was synthesized through the combination of mussel-inspired chemistry and the Michael addition reaction. This modification could be used as an efficient method for improving the dispersion stability of MoS_2 in PAG base oil. The tribological results illustrated that the addition of 0.7 wt% MoS_2–PDA–MGA in PAG was the optimum content to provide significant friction-reducing and AW properties for steel/steel contacts under a load of 100 N at 150 °C. The tribological results of MoS_2–PDA–MGA and MoS_2 dispersed in PAG base oil after settling for 7 days indicate that MoS_2–PDA–MGA, with its good dispersion stability, has stable friction-reducing and AW properties. The tribological testing results demonstrated that MoS_2–PDA–MGA was an effective additive for improving the friction-reducing and AW performance of PAG oil at various temperatures, especially at elevated reaction temperatures. XPS analysis indicated that a boundary lubrication film composed of FeO or Fe_2O_3, FeOOH, $FeSO_4$ or $Fe_2(SO_4)_3$, MoS_2, and C–O binding formed on the worn surface, contributing to the excellent friction-reducing and AW behaviors of MoS_2–PDA–MGA as an additive in PAG base oil at elevated temperature.

Conflicts of interest

There are no conflicts to declare.

Acknowledgements

The authors are thankful for financial support of this work by National Key Basic Research Program of China (973 Program) (No. 2013CB632301) and National Natural Science Foundation of China (NSFC 51475445 and 51775536).

References

1 Z. Z. Wu, D. Z. Wang, Y. Wang and A. K. Sun, *Adv. Eng. Mater.*, 2010, **12**, 534–538.
2 A. Greco, K. Mistry, V. Sista, O. Eryilmaz and A. Erdemir, *Wear*, 2011, **271**, 1754–1760.
3 G. Y. Bai, J. Q. Wang, Z. G. Yang, H. G. Wang, Z. F. Wang and S. R. Yang, *RSC Adv.*, 2014, **4**, 47096–47105.
4 M. Gulzar, H. H. Masjuki, M. Varman, M. A. Kalam, R. A. Mufti, N. W. M. Zulkifli and R. Yunus, *Tribol. Int.*, 2015, **88**, 271–279.
5 N. Salah, M. S. Abdel wahab, A. Alshahrie, N. D. Alharbi and Z. H. Khan, *RSC Adv.*, 2017, **7**, 40295–40302.
6 W. Li, Z. L. Cheng and Z. Liu, *RSC Adv.*, 2016, **6**, 110866–110873.
7 M. Kalin, J. Kogovšek and M. Remškar, *Wear*, 2012, **280**, 36–45.
8 I. Lahouij, B. Vacher, J. M. Martin and F. Dassenoy, *Wear*, 2012, **296**, 558–567.
9 L. N. Zhu, C. B. Wang, H. D. Wang, B. S. Xu, D. M. Zhuang, J. J. Liu and G. L. Li, *Appl. Surf. Sci.*, 2012, **258**, 1944–1948.
10 Y. B. Zhang, C. H. Li, D. Z. Jia, D. K. Zhang and X. W. Zhang, *J. Cleaner Prod.*, 2015, **87**, 930–940.
11 S. Kumari, R. Gusain, N. Kumar and O. Khatri, *J. Ind. Eng. Chem.*, 2016, **42**, 87–94.
12 A. Alazemi, A. Dysart, X. L. Phuah, V. Pol and F. Sadeghi, *Carbon*, 2016, **110**, 367–377.
13 P. U. Aldana, B. Vacher, T. L. Mogne, M. Belin, B. Thiebaut and F. Dassenoy, *Tribol. Int.*, 2014, **56**, 249–258.
14 Z. Chen, X. W. Liu, Y. H. Liu, S. Gunsel and J. B. Luo, *Sci. Rep.*, 2015, **5**, 12869–12876.
15 Z. Y. Xu, Y. Xu, K. H. Hu, Y. F. Xu and X. G. Hu, *Tribol. Int.*, 2015, **81**, 139–148.
16 Q. M. Wan, Y. Jin, P. C. Sun and Y. L. Ding, *J. Nanopart. Res.*, 2014, **16**, 2386–2395.
17 S. Kumari, O. P. Sharma, R. Gusain, H. P. Mungse, A. Kukrety, N. Kumar, H. Sugimura and O. P. Khatri, *ACS Appl. Mater. Interfaces*, 2015, **7**, 3708–3716.
18 P. F. Du, G. X. Chen, S. Y. Song, H. L. Chen, J. Li and Y. Shao, *Tribol. Int.*, 2016, **62**, 29–38.
19 L. Liu, Z. B. Huang and P. Huang, *Tribol. Int.*, 2016, **104**, 303–308.
20 S. K. Madhurakkat Perikamana, J. K. Lee, Y. B. Lee, Y. M. Shin, E. J. Lee, A. G. Mikos and H. Shin, *Biomacromolecules*, 2015, **16**, 2541–2555.
21 K. Chen, X. Q. Xu, J. W. Guo, X. L. Zhang, S. L. Han, R. B. Wang, X. H. Li and J. X. Zhang, *Biomacromolecules*, 2015, **16**, 3574–3583.
22 G. J. Zeng, M. Y. Liu, X. H. Liu, Q. Huang, D. Z. Xu, L. C. Mao, H. Y. Huang, F. J. Deng, X. Y. Zhang and Y. We, *Appl. Surf. Sci.*, 2016, **387**, 399–405.
23 X. J. Zheng, Y. F. Xu, J. Geng, Y. B. Peng, D. Olson and X. G. Hu, *Tribol. Int.*, 2016, **102**, 79–87.
24 X. H. Wu, G. Q. Zhao, Q. Zhao, K. L. Gong, X. B. Wang, W. M. Liu and W. S. Liu, *RSC Adv.*, 2016, **101**, 98606–98610.
25 J. Zhao, Y. Y. He, Y. F. Wang, W. Wang, L. Yan and J. B. Luo, *Tribol. Int.*, 2016, **97**, 14–20.
26 A. Moshkovith, V. Perfiliev, I. Lapsker, N. Fleischer, R. Tenne and L. Rapoport, *Tribol. Int.*, 2006, **24**, 225–228.
27 X. H. Wu, J. M. Liu, Q. Zhao, M. Zhang, G. Q. Zhao and X. B. Wang, *ACS Sustainable Chem. Eng.*, 2015, **3**, 2281–2290.
28 K. H. Hu, X. G. Hu, Y. F. Xu, F. Huang and J. S. Liu, *Tribol. Int.*, 2010, **40**, 225–228.

